Electronic Supplementary Information (ESI)

Soft X-ray Absorption Spectroscopy for Analysing Aluminium Complexes in Solution

Ryota Takahashi,[a] Fumitoshi Kumaki,[b] Jun-ichi Adachi,[b] Yoshihiro Nishimoto,*[a,c,d] Makoto Yasuda,*[a,c] Masanari Nagasaka*[e]

[a]*Department of Applied Chemistry, Graduate School of Engineering, The University of Osaka, 2-1 Yamadaoka, Suita, Osaka 565-0871, Japan. E-mail: nishimoto@chem.eng.osaka-u.ac.jp, yasuda@chem.eng.osaka-u.ac.jp*

[b]*Photon Factory, Institute of Materials Structure Science, High Energy Accelerator Research Organization, 1-1 Oho, Tsukuba, Ibaraki 305-0801, Japan.*

[c]*Innovative Catalysis Science Division, Institute for Open and Transdisciplinary Research Initiatives (ICS-OTRI), The University of Osaka, 2-1 Yamadaoka, Suita, Osaka 565-0871, Japan*

[d]*PRESTO, Japan Science and Technology Agency (JST), Kawaguchi, Saitama 332-0012, Japan.*

[e]*Institute for Molecular Science and Graduate Institute for Advanced Studies, SOKENDAI, Myodaiji, Okazaki 444-8585, Japan. E-mail: nagasaka@ims.ac.jp.*

Contents

General

NMR spectra were recorded on JEOL JNM-ECZL400S spectrometers (103 MHz for ^{27}Al). Chemical shifts were reported in ppm on the δ scale relative to $AlCl_3$ in D_2O ($\delta = 0$ for ^{27}Al NMR) as an external reference. Tris(acetylacetonato)aluminium ($Al(acac)_3$) and diisopropylethylamine (iPr$_2$EtN) was purchased from Tokyo Chemical Industry Co., Ltd. and used as obtained. Al-salen complex, (*R*,*R*)-[1,2-cyclohexane-diamino-*N*,*N*'-bis(3,5-di-*tert*-butylsalicylidene)]aluminium was purchased from BLD Pharmatech Ltd. and used as obtained. Dehydrated solvents were purchased from Kanto Chemical Co., Inc. and used as obtained. The details of apparatus of soft X-ray beamline are described below.

Spectral Processing Method

An example of the data processing procedure is presented.

Sample: Al-salen in THF (Figure 4e)

(step 1) Incident soft X-ray spectrum (I_0) (Figure S1)

(step 2) Raw spectrum of Al-salen in THF (I) (Figure S2)

(step 3) $\ln(I_0/I)$ after referencing absorption energy with Al foil (Figure S3)

(step 4) $\ln(I_0/I)$ with a linear background (Figure S4)

(step 5) $\ln(I_0/I)$ after subtracting a linear background (Figure S5)

* For the Al-salen complex in DMSO, the background was subtracted using two linear baselines.

(step 6) Normalization and $\ln(I_0/I)$ and fittings (Figure S6)

The spectral noise is believed to originate primarily from fluctuations in the soft X-ray beam position. The incident soft X-ray beam intensity (I_0) is measured using a gold mesh, which captures the entire soft X-ray beam and is thus less sensitive to positional fluctuations. In contrast, the transmitted intensity (I) is measured after the beam passes through a 200 μm × 200 μm Si_3N_4 membrane, making it more susceptible to beam position instability. Thus, fluctuations in the incident soft X-ray beam are more strongly reflected in the I signal, resulting in a lower S/N compared to I_0 (See Figure S1 and S2 in the Supporting Information). These fluctuations are considered to be responsible for the background ringing artifacts in the processed spectrum. The spectral noise exhibits a longer periodicity and is not caused by the smoothing procedure. The reason for the poorest S/N observed in the spectrum measured in dichloroethane is likely due either to the measurement having been conducted during a time period with significant beam instability, or to the influence of beam fluctuations being more pronounced due to variations in the thickness of the liquid cell.

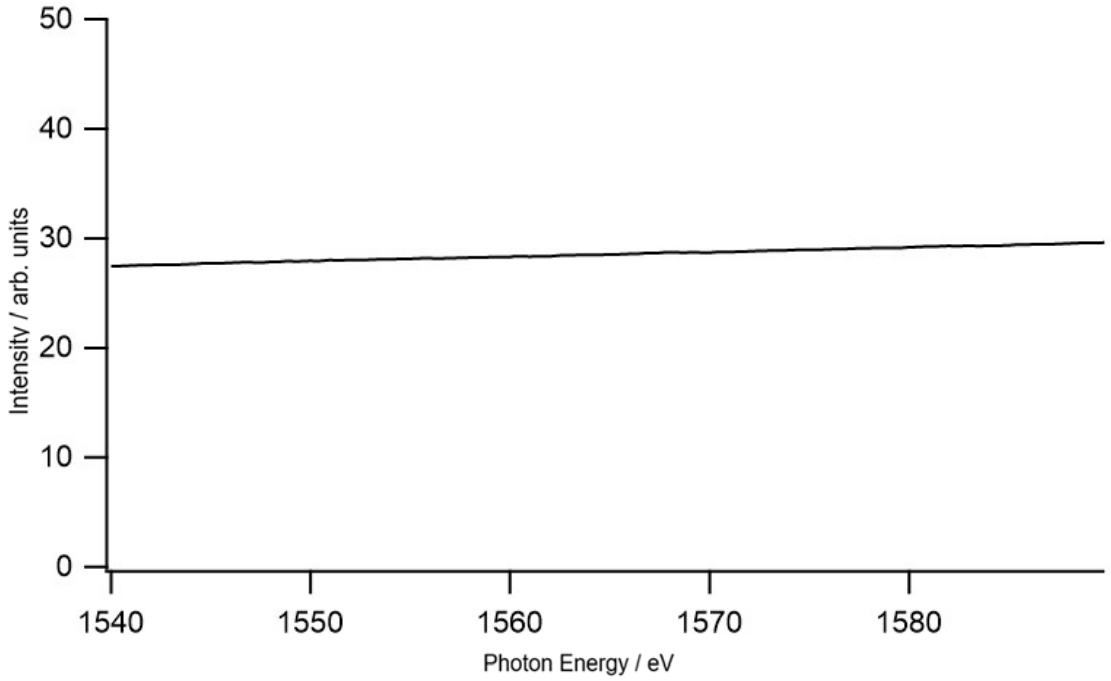

Figure S1. Incident soft X-ray spectrum (I_0)

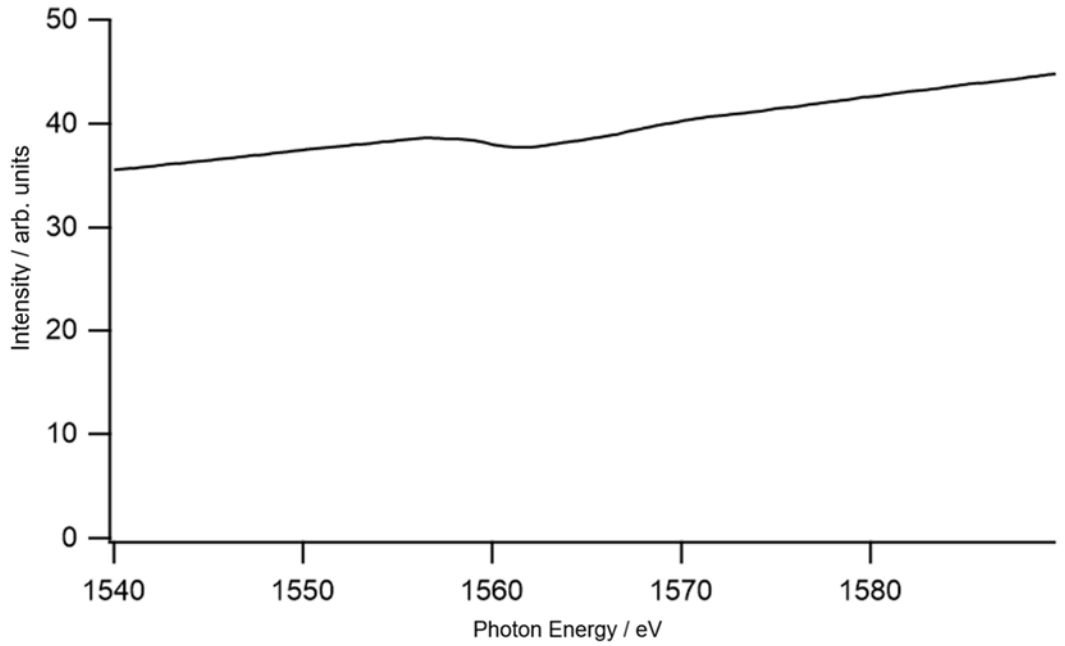

Figure S2. Raw spectrum of Al-salen in THF (I)

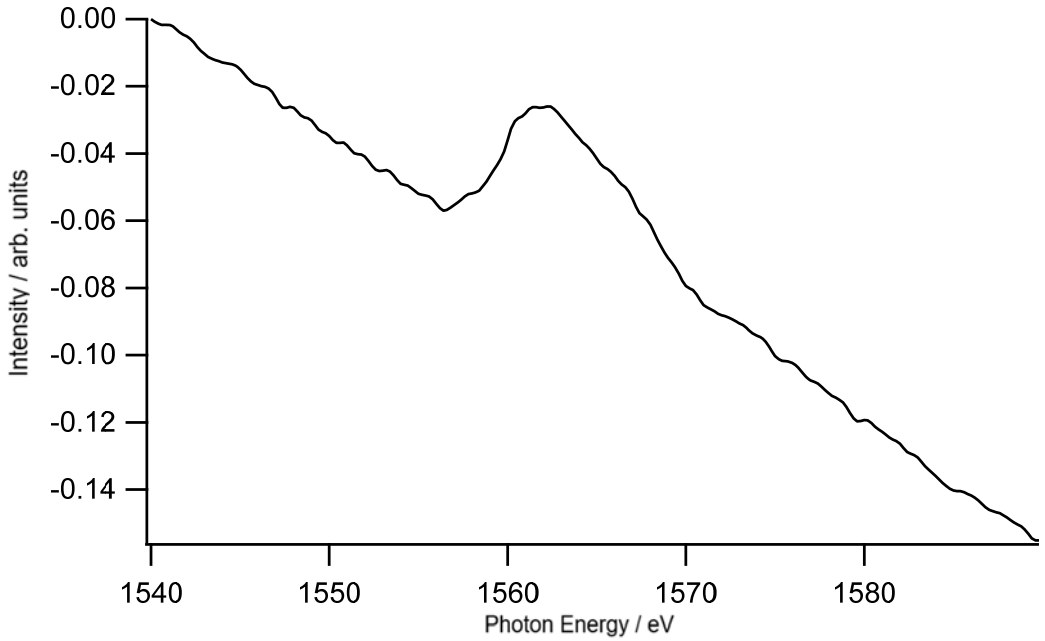

Figure S3. ln(I_0/I) after referencing absorption energy with Al foil

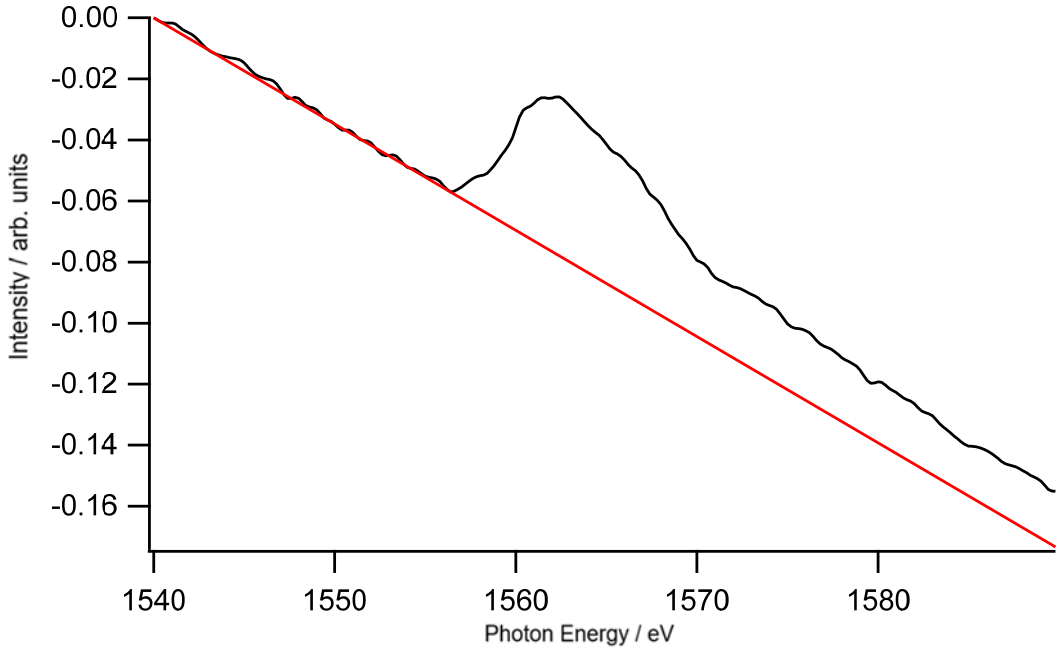

Figure S4. ln(I_0/I) with a linear background

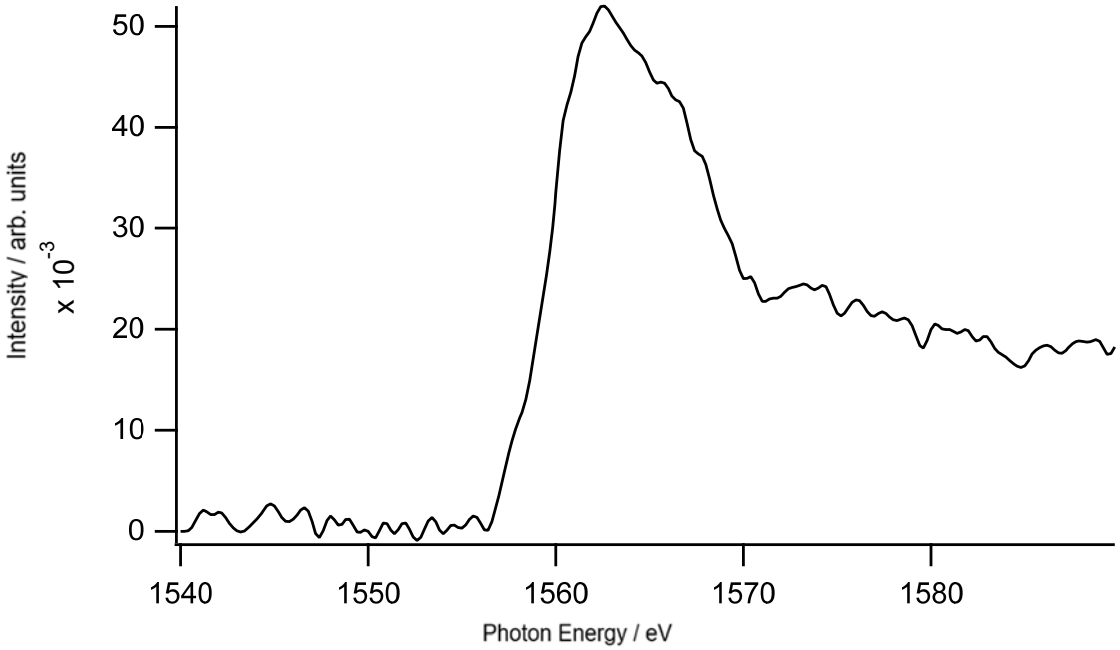

Figure S5. ln(I_0/I) after subtracting a linear background

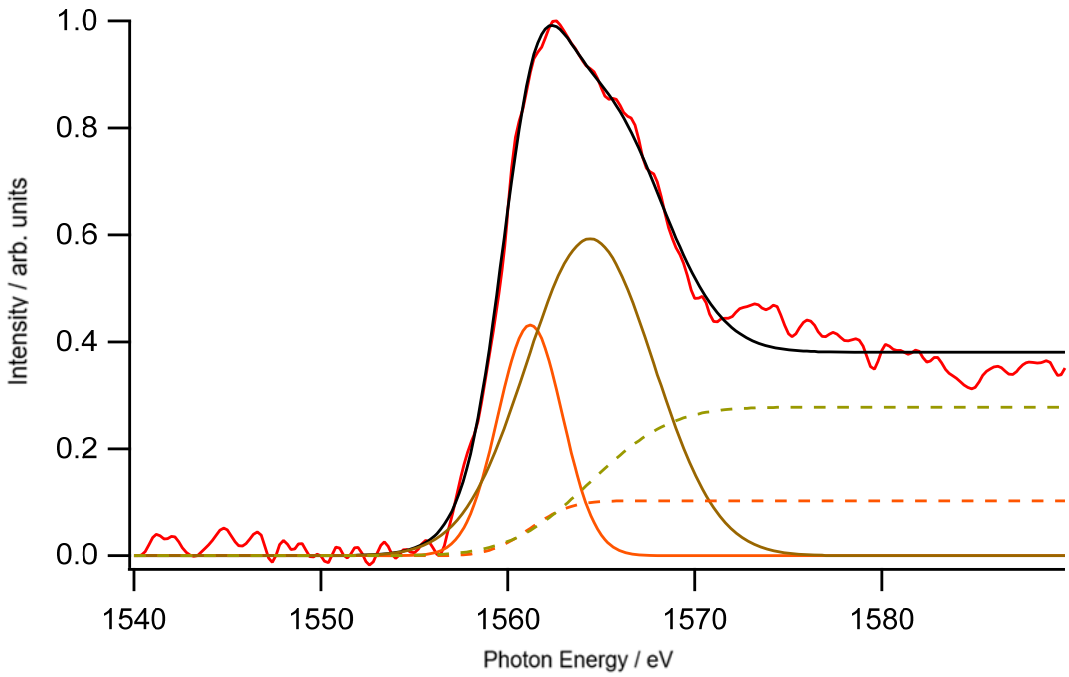

Figure S6. Normalized ln(I_0/I) and fittings

XAS Edge-step and White-line Fitting

Based on previously reported methods,[1-3] with slight modifications, we analyzed the Al *K*-edge soft X-ray absorption spectra by modeling the edge step as the error function (erf) and the white-line as a Gaussian peak. The erf step is the cumulative distribution of a Gaussian and therefore corresponds to an ideal Heaviside step broadened by Gaussian instrumental/inhomogeneous effects.

Model

For one component, the spectral intensity is

$$I(E) = S(E; A, P, W) + G(E; A_g, P, \sigma) + C,$$

with

$$S(E; A, P, W) = A\left[\tfrac{1}{2} + \tfrac{1}{2}\,\mathrm{erf}\left(\frac{E - P}{W/(2\sqrt{\ln 2})}\right)\right], \qquad G(E; A_g, P, \sigma) = A_g \exp\left[-\frac{(E-P)^2}{2\sigma^2}\right].$$

The step width W and Gaussian width σ are linked by

$$W = 2\sqrt{2\ln 2}\,\sigma \equiv \mathrm{FWHM},$$

and the Gaussian center is constrained to the step inflection point,

$$P_{\mathrm{Gaussian}} = P_{\mathrm{step}} \equiv P.$$

For the two-component model used in this work (edge + shoulder), the total signal is the sum of two such pairs (indexed by i = 1, 2):

$$I(E) = \sum_{i=1}^{2} \left\{ S(E; A_i, P_i, W_i) + G\big(E; A_{g,i}, P_i, \sigma_i\big) \right\} + C,$$

with the same center/width link $W_i = 2\sqrt{2\ln 2}\,\sigma_i$.

Additionally, we enforced that the Gaussian peak-area ratio equals the step-height ratio:

$$\frac{\int G_1\,dE}{\int G_2\,dE} = \frac{A_{g,1}\sigma_1\sqrt{2\pi}}{A_{g,2}\sigma_2\sqrt{2\pi}} = \frac{A_1}{A_2} \quad \Rightarrow \quad A_{g,1} = A_{g,2}\,\frac{\sigma_2}{\sigma_1}\,\frac{A_1}{A_2}.$$

Unless otherwise stated, the constant offset was fixed to zero after normalization (C = 0).

Normalization

Spectra were normalized to the edge jump determined from the step part of the model. Pre-edge and post-edge baselines were estimated far below and above the edge, respectively, and the data were scaled as

$$\mu_{\mathrm{norm}}(E) = \frac{\mu(E) - \mu_{\mathrm{pre}}}{\mu_{\mathrm{post}} - \mu_{\mathrm{pre}}}$$

.

Fitting was then performed on the unshifted but normalized $\mu(E)$ with C = 0.

Fitting procedure

Initial edge positions P_i were obtained from the maximum of the smoothed numerical derivative. Step heights A_i were initialized from the difference between post-edge and pre-edge medians; initial σ_i were set to a few eV. Non-linear least-squares with bound constraints was used to optimize all free parameters under the links above. Parameter uncertainties were taken from the covariance matrix. As a sensitivity check, we also fitted a reduced model (erf step ×1 + Gaussian ×1) with the same center/width constraint.

This approach provides a physically motivated decomposition in which (i) the step captures the continuum edge jump and (ii) the Gaussian(s) quantify the white-line peak(s), while keeping peak positions and broadenings internally consistent.

Al K-edge XAS Spectra of $Al(acac)_3$

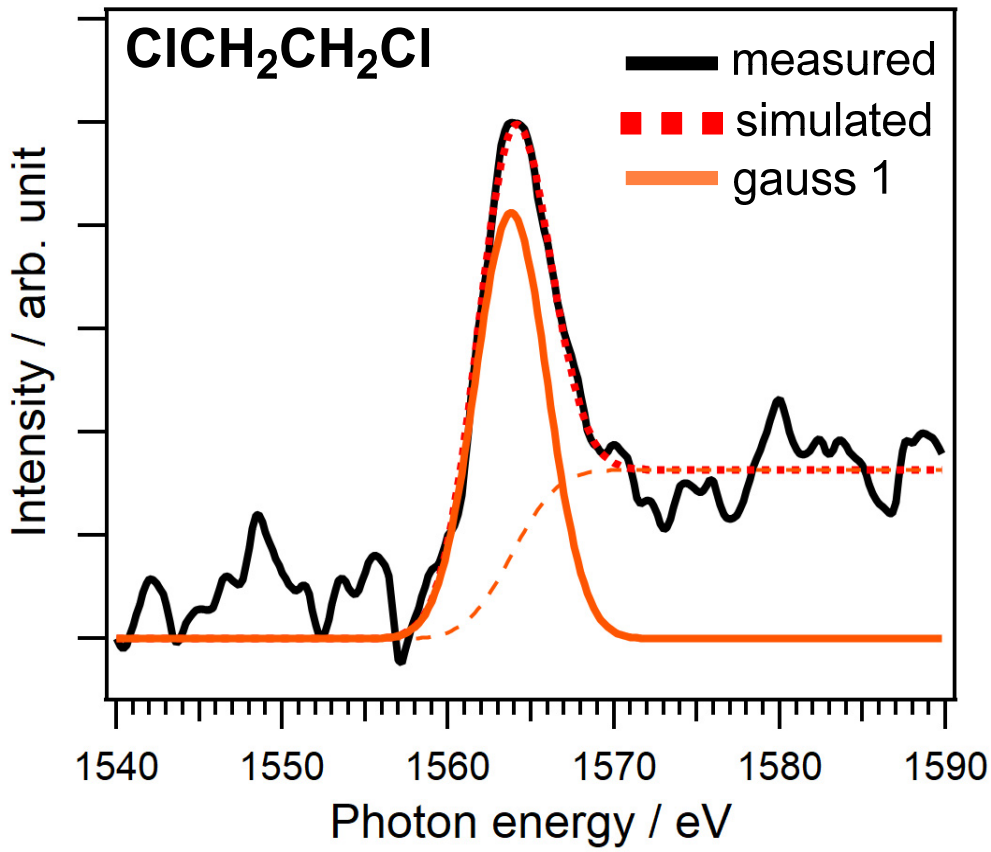

Figure S7. Al K-edge XAS spectrum of $Al(acac)_3$ (black solid line), and the simulated spectrum (red dotted), which is composed of a set of Gaussian function and erf step (orange solid and orange broken).

Fitting Parameter

P/ eV: 1563.8

A: 0.32733

σ/ eV: 2.1751

W/ eV: 5.122085994

A_g: 0.82508

Offset_*C*: 0

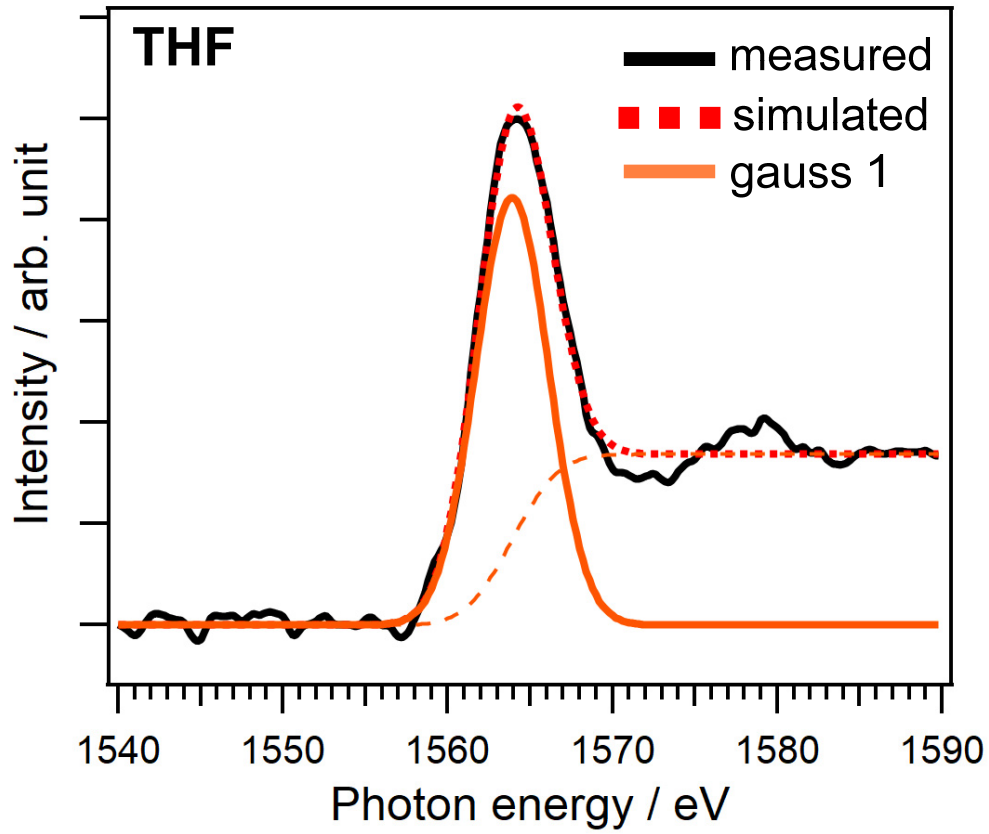

Figure S8. Al K-edge XAS spectrum of $Al(acac)_3$ (black solid line), and the simulated spectrum (red dotted), which is composed of a set of Gaussian function and erf step (orange solid and orange broken).

Fitting Parameter

P/ eV: 1563.9

A: 0.33745

σ/ eV: 2.2094

W/ eV: 5.2027

A_g: 0.84519

Offset_*C*: 0

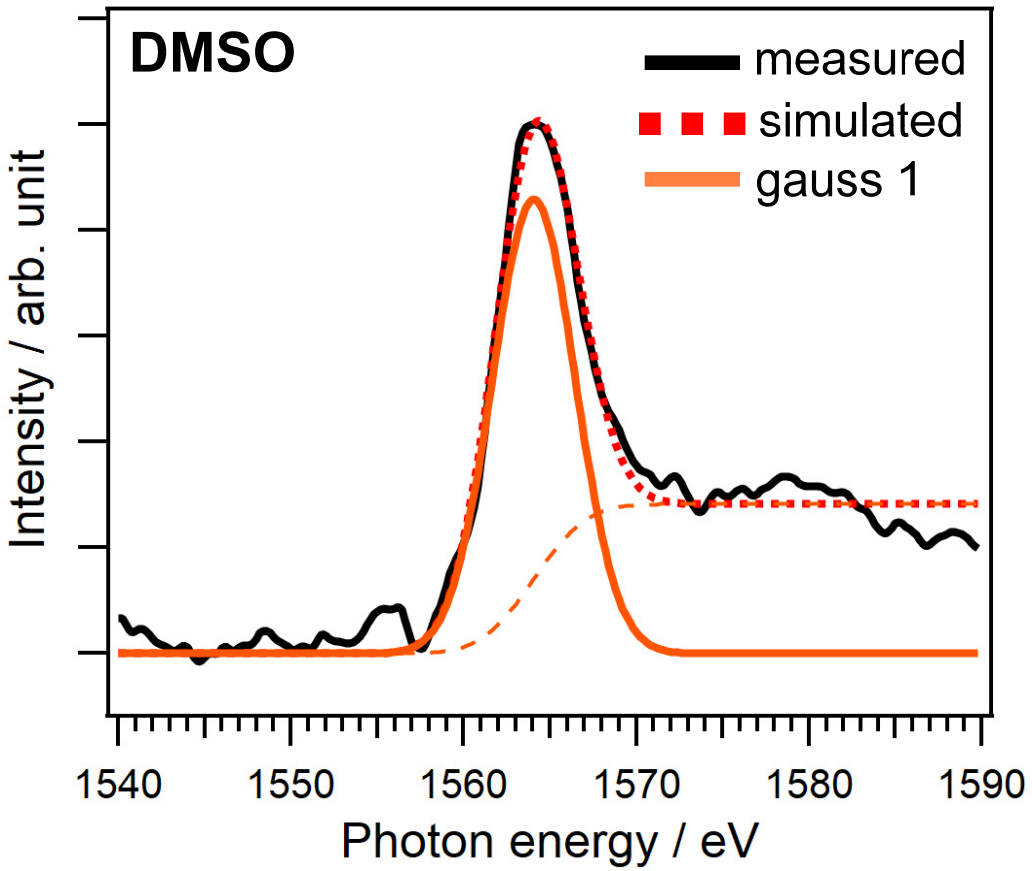

Figure S9. Al K-edge XAS spectrum of $Al(acac)_3$ (black solid line), and the simulated spectrum (red dotted), which is composed of a set of Gaussian function and erf step (orange solid and orange broken).

Fitting Parameter

P/ eV: 1564.1

A: 0.28266

σ/ eV: 2.3942

W/ eV: 5.6378

A_g: 0.85864

Offset_*C*: 0

Overlaid spectra

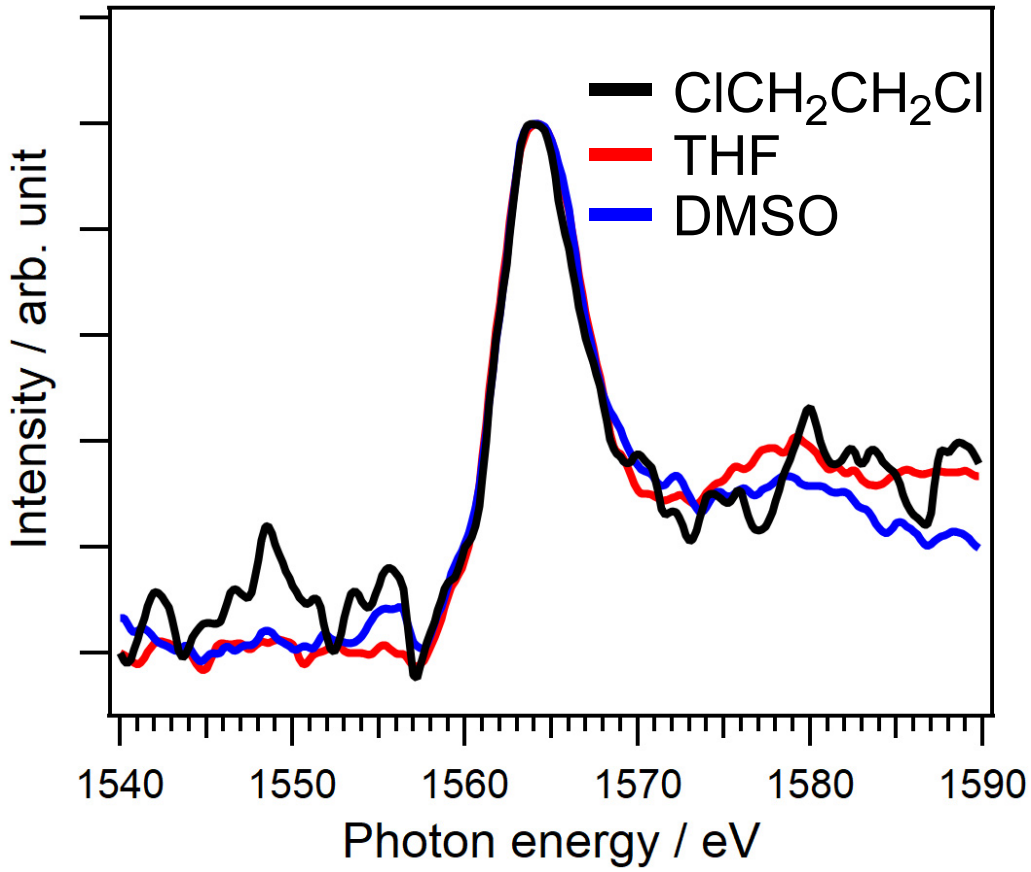

Al K-edge XAS Spectra of Al-salen A

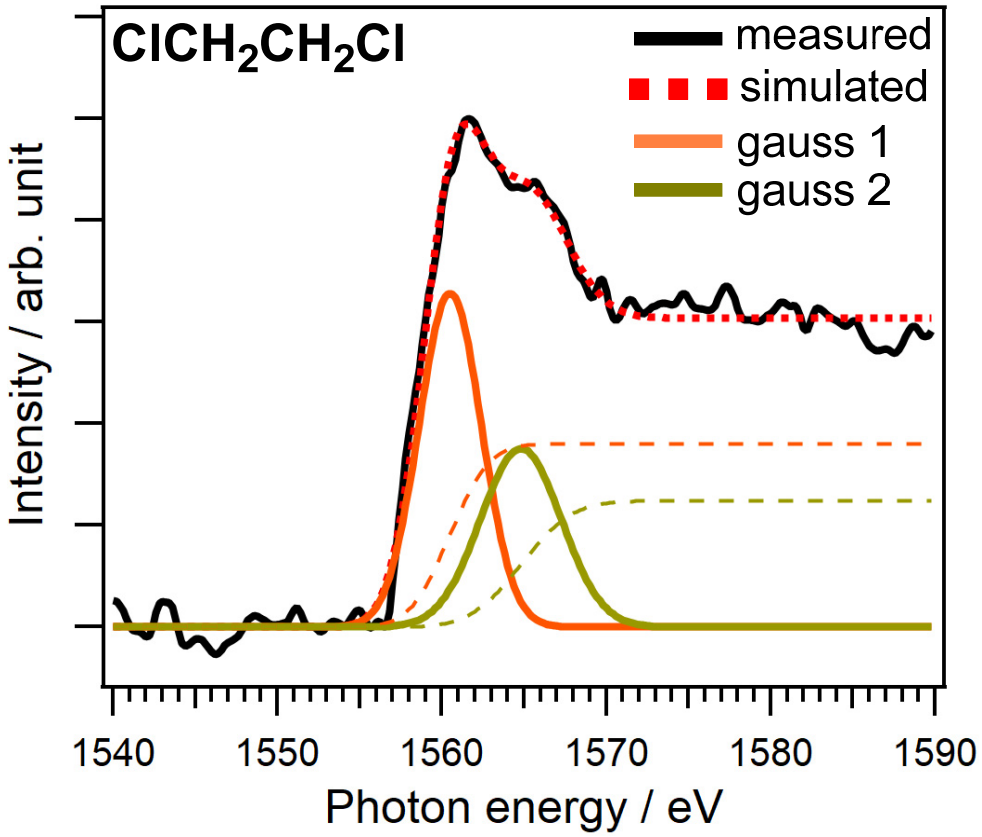

Figure S10. Al K-edge XAS spectrum of **A** (black solid line), and the simulated spectrum (red dotted), which is composed of one or two sets of Gaussian function and erf step (orange/ochre solid and orange/ochre broken).

Fitting Parameter

P_1/ eV: 1560.5

P_2/ eV: 1564.8

A_1: 0.36000

A_2: 0.24808

σ_1/ eV: 1.8995

σ_2/ eV: 2.4500

W_1/ eV: 4.4731

W_2/ eV: 5.7692

$A_{g,1}$: 0.65716

$A_{g,2}$: 0.35111

Area_gauss 1/3.1290

Area_gauss 2/2.1562

Offset_C: 0

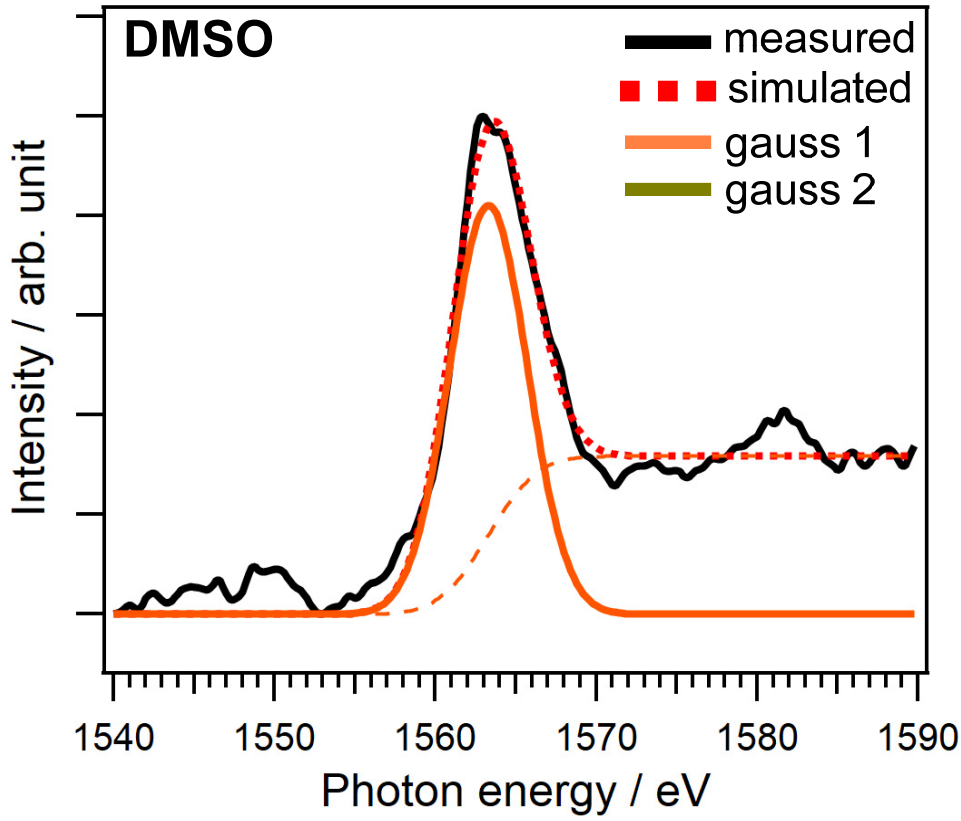

Figure S11. Al K-edge XAS spectrum of **A** (black solid line), and the simulated spectrum (red dotted), which is composed of a set of Gaussian function and erf step (orange solid and orange broken).

Fitting Parameter

P/ eV: 1563.3

A: 0.31794

σ/ eV: 2.4321

W/ eV: 5.7273

A_g: 0.80724

Offset_*C*: 0

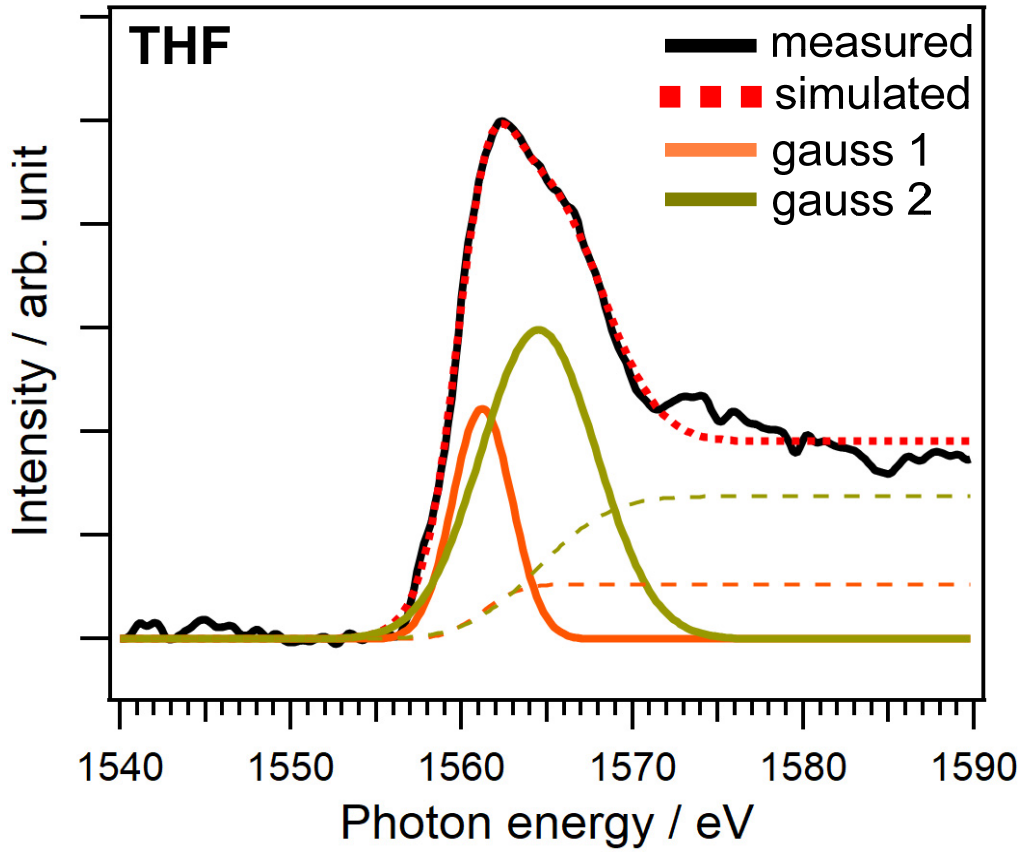

Figure S12. Al K-edge XAS spectrum of **A** (black solid line), and the simulated spectrum (red dotted), which is composed of one or two sets of Gaussian function and erf step (orange/ochre solid and orange/ochre broken).

Fitting Parameter

P_1/ eV: 1561.2

P_2/ eV: 1564.4

A_1: 0.10285

A_2: 0.27783

σ_1/ eV: 1.7304

σ_2/ eV: 3.4025

W_1/ eV: 4.0748

W_2/ eV: 8.0123

$A_{g,1}$: 0.43143

$A_{g,2}$: 0.59269

Area_gauss 1/0.59269

Area_gauss 2/5.0549

Offset_C: 0

Overlaid spectra

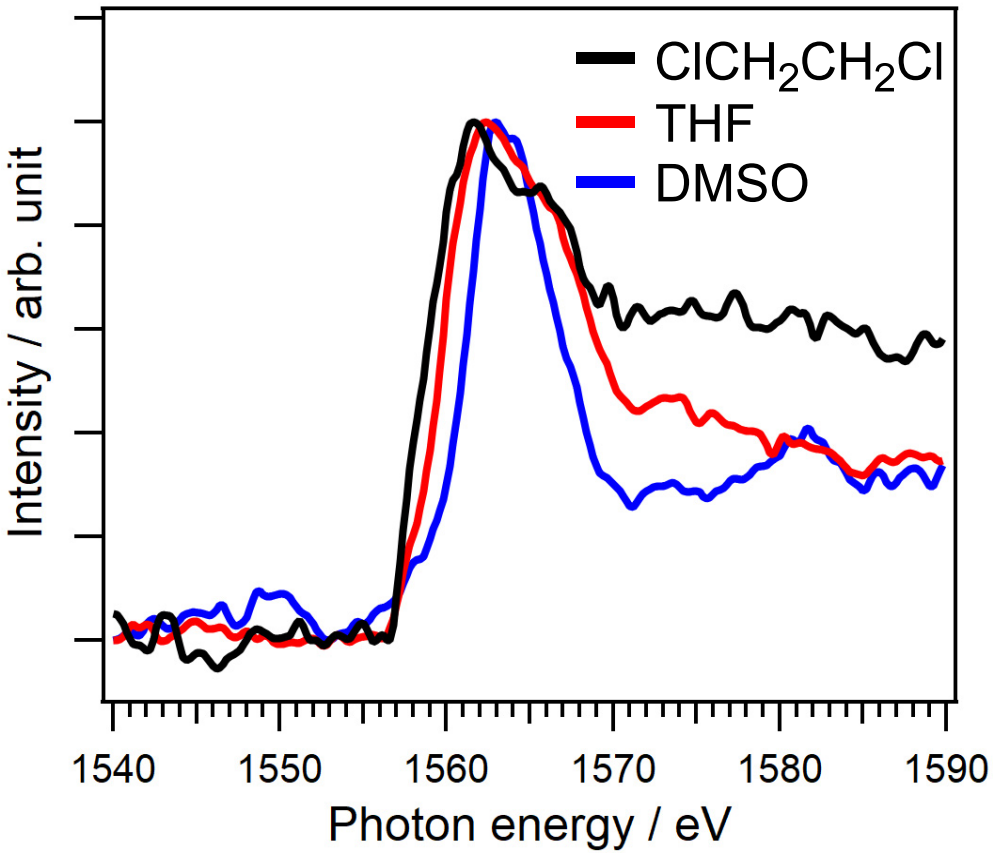

Al K-edge XAS Spectra of Al-salen (A) with *i*Pr$_2$EtN

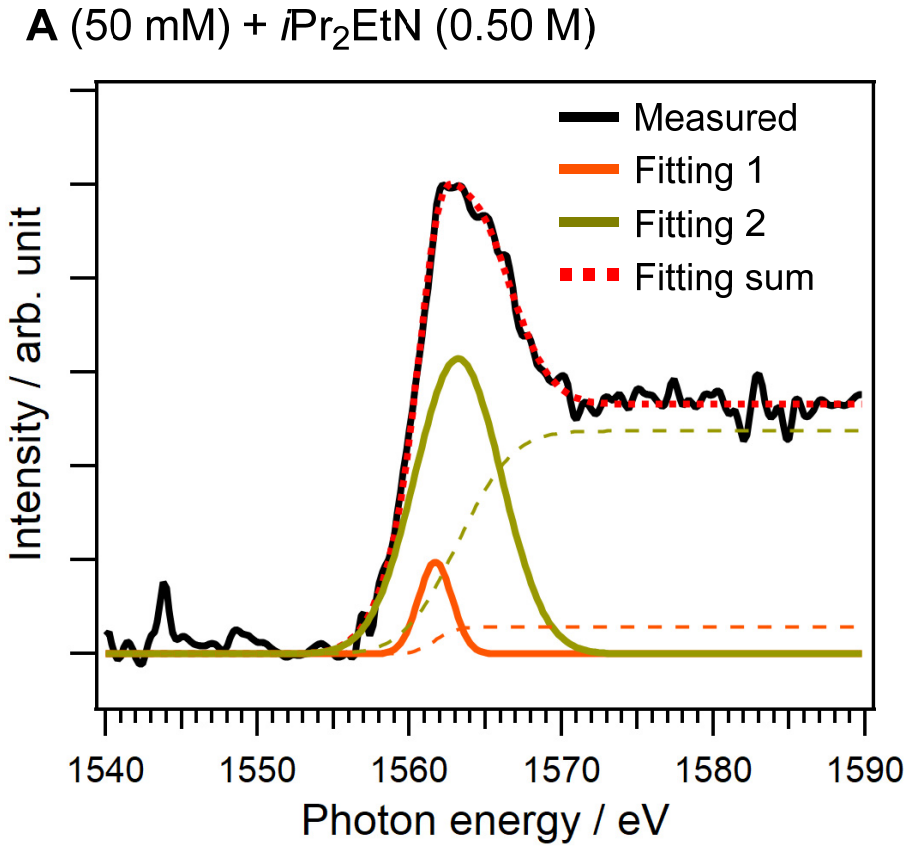

Figure S13. Al K-edge XAS spectrum of **A** (black solid line), and the simulated spectrum (red dotted), which is composed of one or two sets of Gaussian function and erf step (orange/ochre solid and orange/ochre broken).

Fitting Parameter

P_1/ eV: 1561.7

P_2/ eV: 1563.2

A_1: 0.057466

A_2: 0.47497

σ_1/ eV: 1.0985

σ_2/ eV: 2.8368

W_1/ eV: 2.5868

W_2/ eV: 6.6800

$A_{g,1}$: 0.19669

$A_{g,2}$: 0.62950

Area_gauss 1/0.54157

Area_gauss 2/4.4761

Offset_C: 0

Overlaid spectra

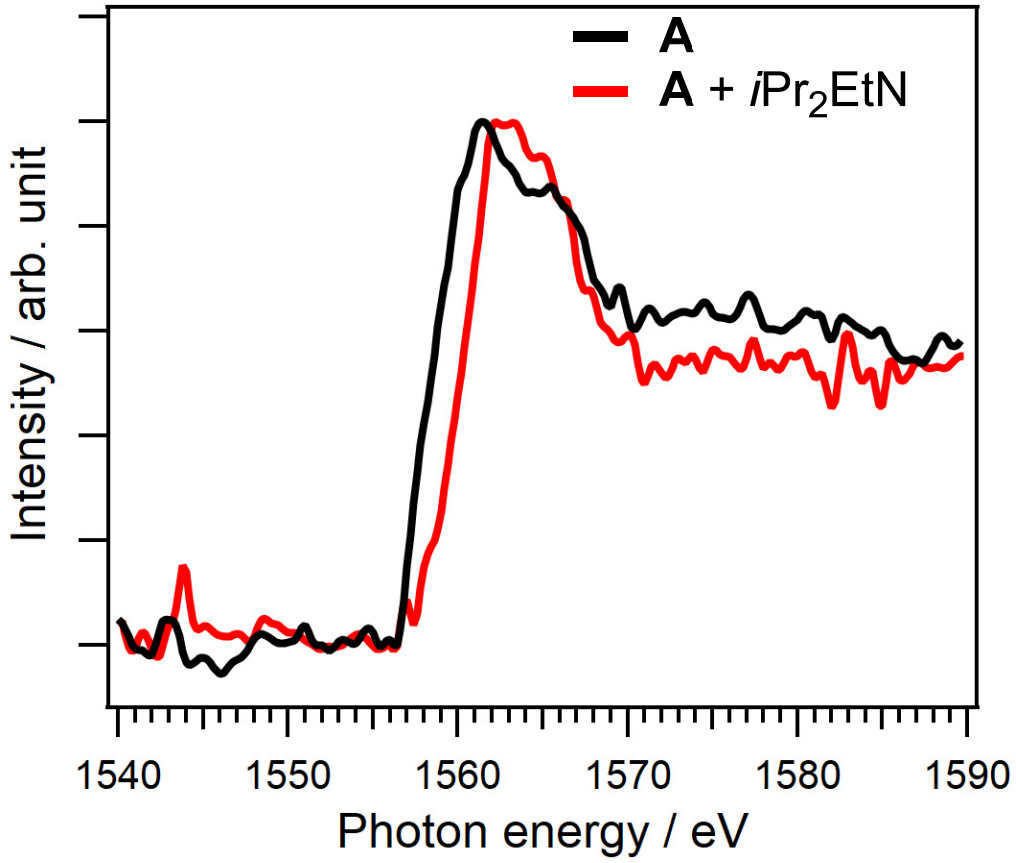

^{27}Al NMR Spectroscopy

Al(acac)$_3$ in ClCH$_2$CH$_2$Cl (50 mM)

^{27}Al{^{1}H} NMR: (103 MHz, AlCl$_3$ in D$_2$O as an external standard)

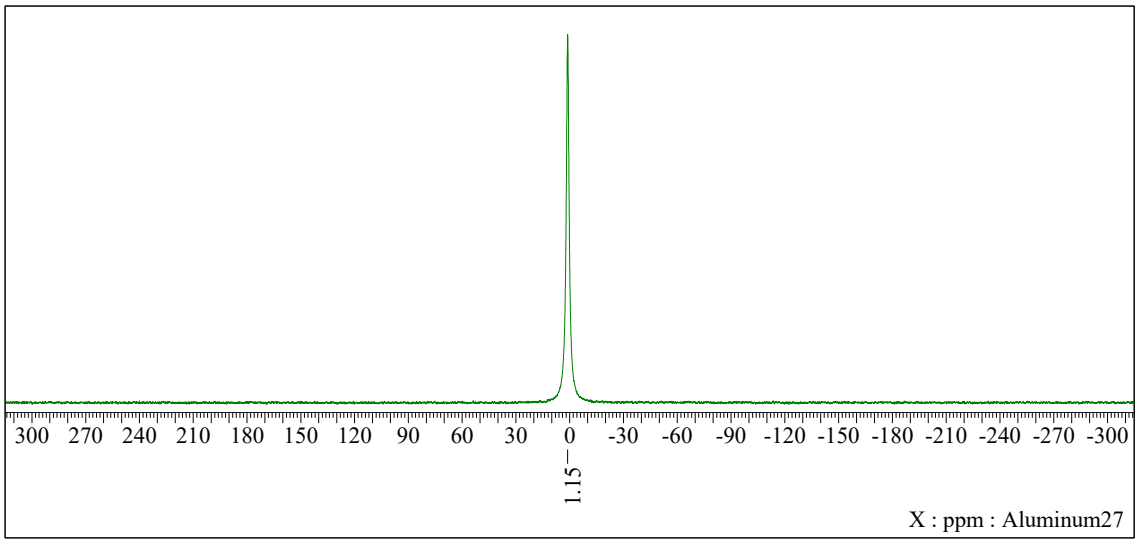

Al(acac)$_3$ in THF (50 mM)

^{27}Al{^{1}H} NMR: (103 MHz, AlCl$_3$ in D$_2$O as an external standard)

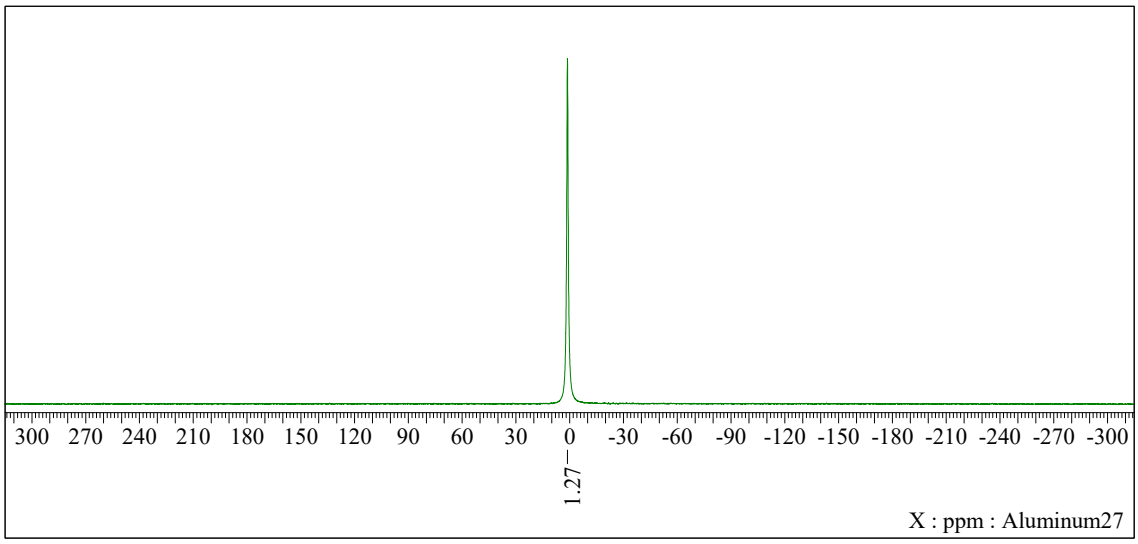

$Al(acac)_3$ in DMSO (50 mM)

$^{27}Al\{^{1}H\}$ NMR: (103 MHz, $AlCl_3$ in D_2O as an external standard)

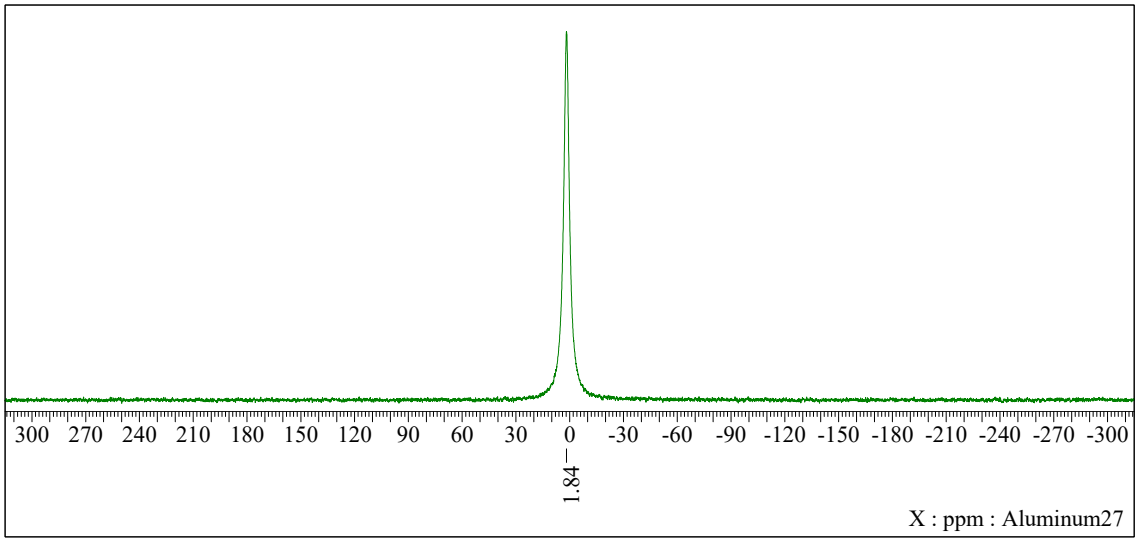

Overlaid ^{27}Al NMR spectra of $ClCH_2CH_2Cl$, THF, and DMSO solution of $Al(acac)_3$

Green: $ClCH_2CH_2Cl$, Blue: THF, Brown: DMSO

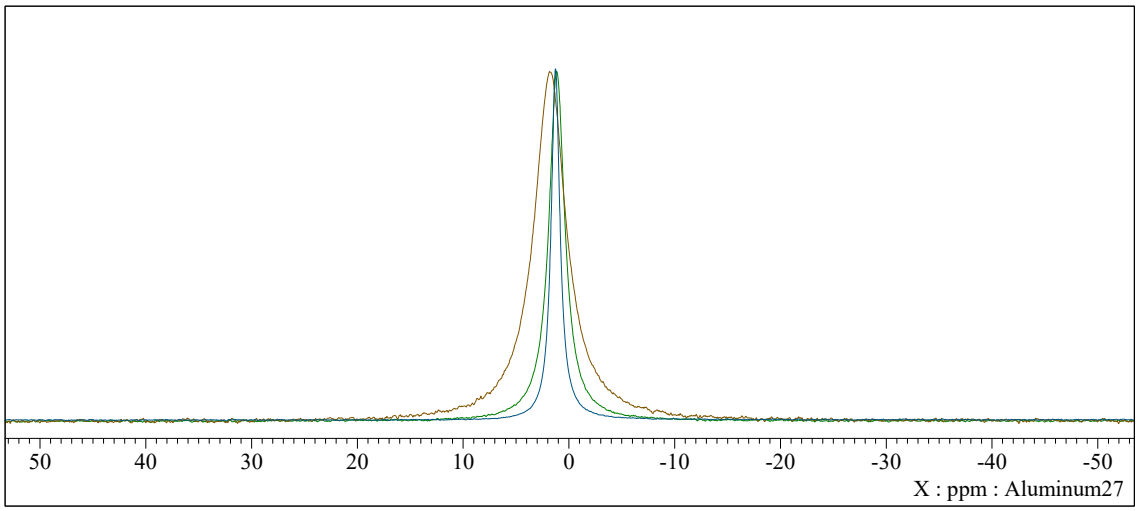

Al-salen (A) in $ClCH_2CH_2Cl$ (50 mM)

$^{27}Al\{^{1}H\}$ NMR: (103 MHz, $AlCl_3$ in D_2O as an external standard)

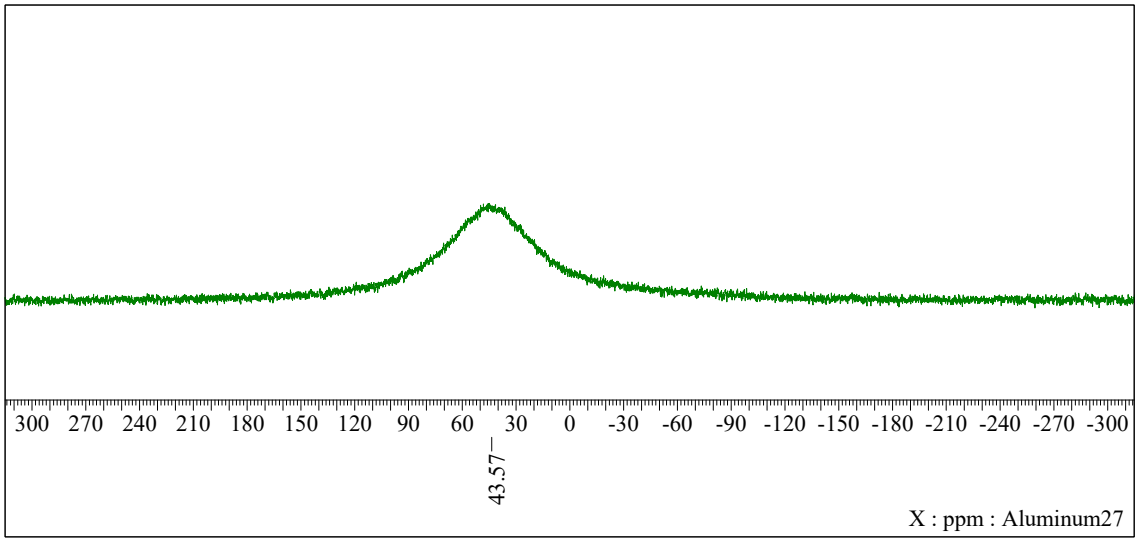

Al-salen (A) in THF (50 mM)

$^{27}Al\{^{1}H\}$ NMR: (103 MHz, $AlCl_3$ in D_2O as an external standard)

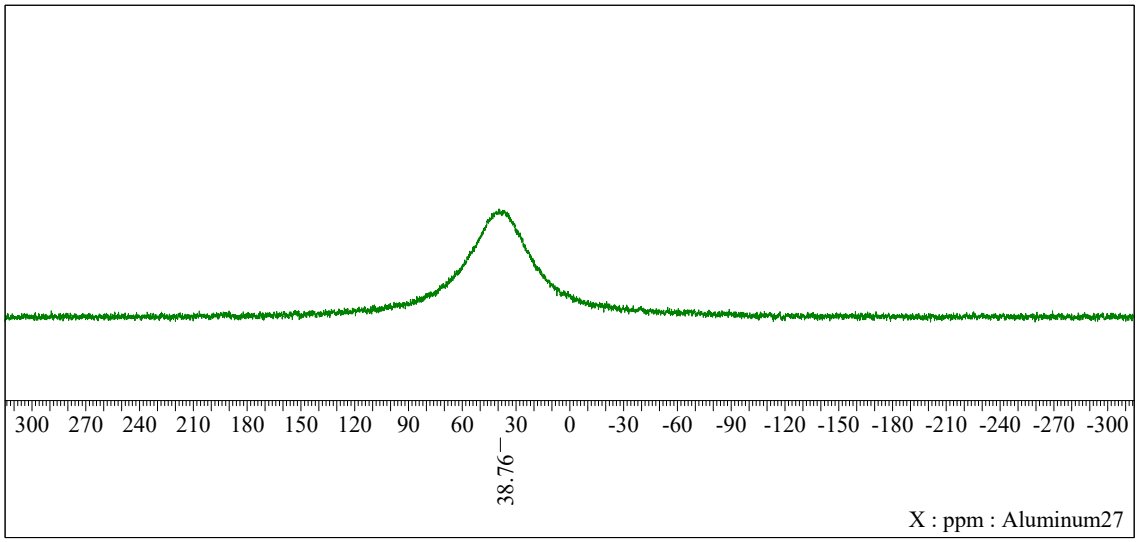

Al-salen (A) in DMSO (50 mM)

$^{27}Al\{^{1}H\}$ NMR: (103 MHz, $AlCl_3$ in D_2O as an external standard)

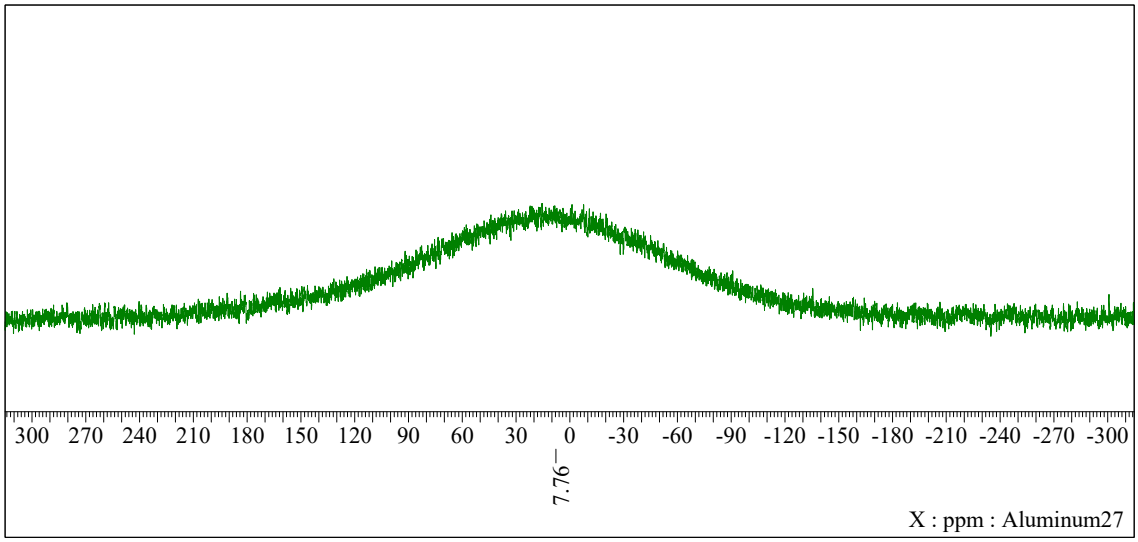

Overlaid ^{27}Al NMR spectra of $ClCH_2CH_2Cl$, THF, and DMSO solution of Al-salen

Blue: $ClCH_2CH_2Cl$, Green: THF, Brown: DMSO

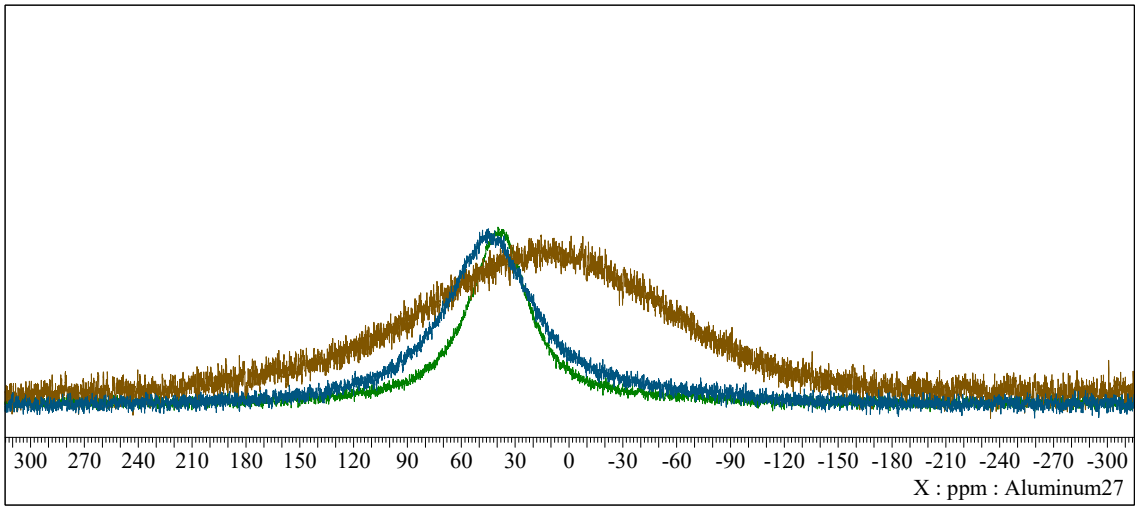

Al-salen (A) (50 mM) + *i*Pr$_2$EtN (500 mM) in ClCH$_2$CH$_2$Cl

^{27}Al{^{1}H} NMR: (103 MHz, $AlCl_3$ in D_2O as an external standard)

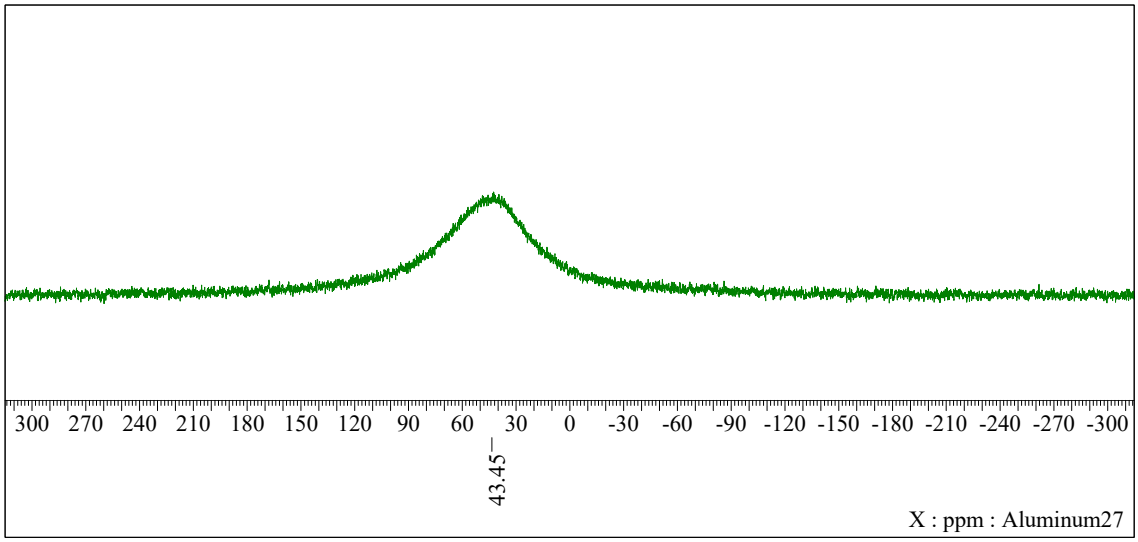

Overlaid ^{27}Al NMR spectra of ClCH$_2$CH$_2$Cl solution of Al-salen with/without *i*Pr$_2$EtN

Green: without *i*Pr$_2$EtN, Brown: with *i*Pr$_2$EtN

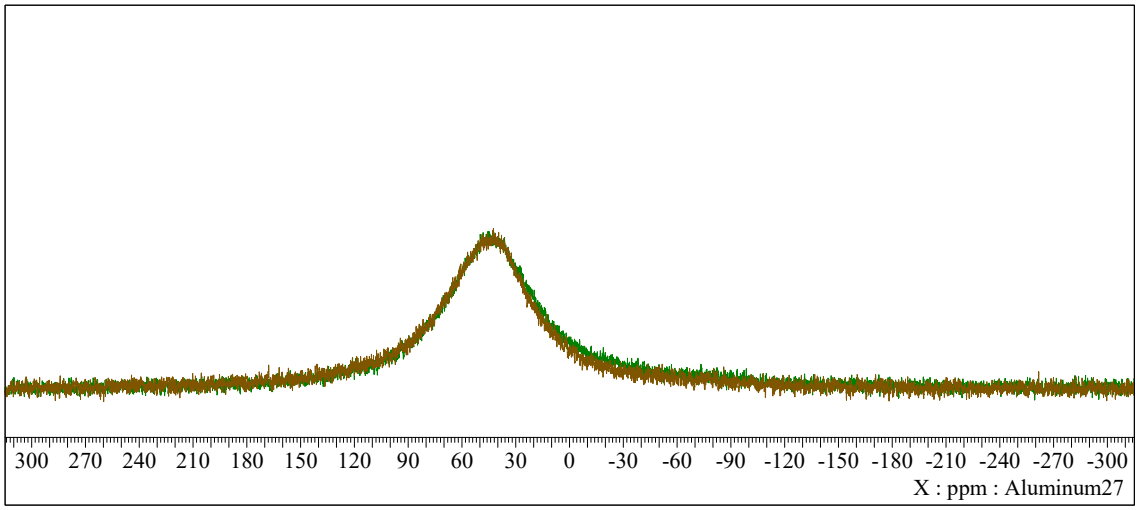

References

1 K. Nishi, K. Shimizu, M. Takamatsu, H. Yoshida, A. Satsuma, T. Tanaka, S. Yoshida, T. Hattori, *J. Phys. Chem. B* 1998, **102**, 10190–10195

2 K. Shimizu, M. Takamatsu, K. Nishi, H. Yoshida, A. Satsuma, T. Tanaka, S. Yoshida, T. Hattori, *J. Phys. Chem. B* 1999, **103**, 1542–1549.

3 K. Shimizu, Y. Kato, T. Yoshida, H. Yoshida, A. Satsuma, T. Hattori, *Chem. Commun.* 1999, 1681–1682.